ICC
Iranian Chemical Communication
Original Research Article
Payame Noor University http://icc.journals.pnu.ac.ir

An investigation on absorption properties of exfoliated graphite for oil spill from Caspian Sea water

Omid Ghasemi[a], Naser Mehrdadi[b,*], Majid Baghdadi[c], Behnoush Aminzadeh[d]

[a]*PhD Candidate, School of Environment, College of Engineering, University of Tehran, Tehran, Iran*

[b]*Professor, School of Environment, College of Engineering, University of Tehran, Tehran*

[c]*Associate Professor, School of Environment, College of Engineering, University of Tehran, Tehran, Iran*

[d]*Assistant Professor, School of Environment, College of Engineering, University of Tehran, Tehran, Iran*

Received: 8 January 2019, Accepted: 30 January 2019, Published: 1 July 2019

Abstract

Oil spills have the most important environmental impact in oceans and seas. In this article, oil absorption, which was explored from Sardar-e-Jangal oilfield in Caspian Sea by exfoliated graphite (EG), was investigated. Graphite was exfoliated through the reaction of graphite-CrO_3 intercalation compounds with hydrogen peroxide. The obtained absorbent was characterized by Brunauer-Emmett-Teller (BET), Fourier transform infrared spectrometer (FT-IR), X-ray Diffraction (XRD), RAMAN spectroscopy, scanning electron microscopy (SEM), and Energy-dispersive X-ray spectroscopy (EDS). Absorption capacity was investigated by response surface methodology (RSM) using design expert data analysis. EG absorbed oil sample from aqueous solution to a great extent as it was due to increasing total pore volume in its structure in comparison to the simple graphite. RSM model fitting and its validation was discussed. Identified parameters (weight of absorbent and oil) were investigated by RSM using Perturbation diagram, contour and 3D surface response plots and the maximum absorption ratio was 27.6 gram (g) oil/gram (g) absorbent. The finding presented herein indicated that EG was successfully used in oil removal from seawater due to its easy synthesis, low cost and high sorption performance.

Keywords: Absorption; Caspian Sea; exfoliated graphite; oil spill; response surface methodology.

Introduction

Petroleum hydrocarbons are the most common environmental pollutants, and oil spills pose a great hazard to terrestrial and marine ecosystems. Oil pollution may arise either accidentally or operationally whenever oil is produced, transported, stored, processed or used at sea or on land. Oil spills are a major menace to the environment because they severely damage the surrounding ecosystems [1-4].

*Corresponding author: Naser Mehrdadi
Tel: +98 (912) 1001255, Fax: +98 (011) 34622668
E-mail: mehrdadi@ut.ac.ir

The Caspian Sea, the biggest enclosed body of water on the Earth, has attracted the attention of the international oil and gas industry. Due to the recent urban development and increasing industrial and oil production activities in the coastal regions of Caspian Sea, considerable amounts of petroleum products are discharged into this marine environment [5-7]. Making operational decisions to prevent possible impacts is inevitable. Large scale disasters, which happened on the fixed offshore platform of "Guneshli" oilfield of Caspian Sea in 2015, confirm that [8].

The goal of any response strategy during oil spill accidents is to select the effective and efficient countermeasures that minimize the overall impact of the oil spill on the environment. Several interactions could be taken to alleviate oil spill problems in the seas and oceans [9]:

- ✓ Oil spill recovery skimmers and booms (Mechanical)
- ✓ Using dispersants (chemical)
- ✓ Using absorbents (physical - to remove remained oil spills)

Among the methods suggested for removing remained oil spills, absorption has attracted the most attention, with a compelling need to find the most appropriate absorbent, including wool, vegetable fiber, zeolite, sawdust, and wood fiber. Although these absorbents possess microporous structures, they have low oil absorption capacity and poor selectivity. For efficient oil absorption, absorbents should have a high specific surface area, hydrophobic and oleophilic surface chemical properties, and proper chemical stability. Over the years, graphite has received considerable attention on account of its favorable properties, including high surface area, excellent electrical conductivity, and high thermal and chemical stability [10].

Expanded graphite's also termed as exfoliated graphite's (EG) are interesting materials for many applications. As a new carbon material, EG has been used in many fields, such as flexible foils, thermal insulators, conductive resin composites, electrodes and electrochemical applications. In the 1990–2000s they also attracted attention as promising sorbents for liquids such as heavy oils. The high sorption capacity is related to EG's textural characteristics and low bulk density. Exfoliation of graphite is a well-known process first observed in 19th century by Schafhaeutl [11-15].

Usually the product, EG, is prepared from graphite intercalation compounds (GICs). The most important ones are the nature of the graphite used for GIC preparation and the nature of the intercalant. Interestingly, GIC stage (the number of carbon layers separating two successive layers of intercalant) seems to have no influence on the exfoliation character. Possible mechanisms of exfoliation have been discussed in a number of works [11]. EG may be obtained from GIC with various intercalated Substances such as CrO_3, H_2SO_4 and etc. in presence of an oxidizer such as H_2O_2,HNO_3, $KMnO_4$ and $FeCl_3$[16-18].

The design of experiment (DOE) can be regarded as the optimization of the experimental effort needed to distinguish parameters influencing the process. Response surface methodology (RSM) is a statistical procedure commonly applied for optimization studies in general and especially in absorbance conditions. There is, therefore, a need to study and optimize the absorbance conditions for a better understanding of the absorption mechanism(s). Commonly, RSM is

utilized for mapping a response surface over a special region of concern, or for selecting operating conditions to obtain purpose requirements. Implementing RSM provides the extension of the parameter space studied and concurrently decreasing the number of experiments [19-22].

In this paper, Exfoliated graphite was synthetized and used as an absorbent for the Caspian Sea oil sample from aqueous solution. Characterizations was investigated by microscopic analysis instruments and the effects of experimental parameters such as weight of EG (g) and weight of oil (g)was discussed using response surface methodology.

Experimental Procedure

Materials

Both natural graphite and hydrochloric acid (HCl 99%) were purchased from Merck (Darmstadt, Hesse, Germany). Chromium trioxide (CrO_3 99%) and hydrogen peroxide (H_2O_2 30%) were provided from Sigma-Aldrich (Saint Louis, MO, USA). The oil used in this study was obtained from Khazar Exploration and production company (KEPCO) (Sardar-e-Jangal Oilfield – Caspian Sea) (API =38.0, specific gravity = 0.83) The Oil properties are provided in Table 1 and Figure 1.

Table 1. Oil sample properties

Specification	Unit	Qty
Specific Gravity @ 15.56 C^0	-	0.8349
API^0	-	38.0
Sulphur Content	Wt.%	0.016
Water Content	Vol%	<0.025
Salt Content	P.T.B.	13
Pour Point	C^o	7
Asphaltenes	Wt.%	<0.5
Wax Content	Wt.%	13.0
Acidity Total	mgKOH/g	0.01
Nickel	mg/L	4
Vanadium	mg/L	<3
Iron	mg/L	4.6
Sodium	mg/L	9.6

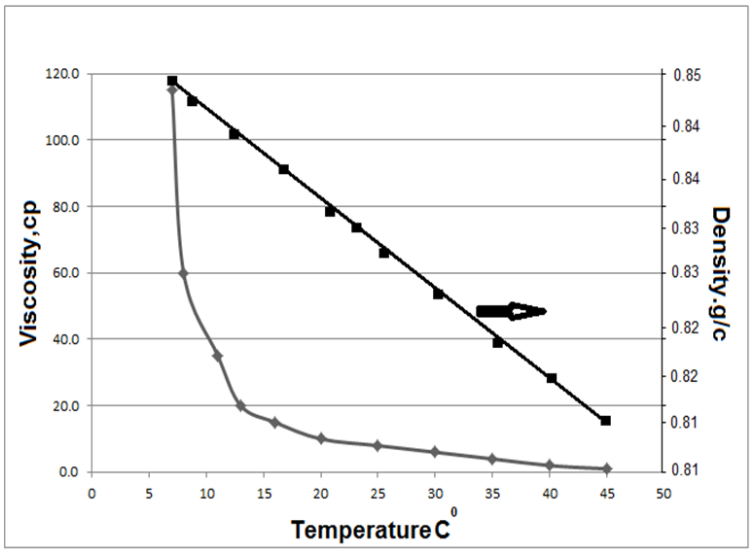

Figure 1. Oil sample viscosity and density changes vs. temperature

Exfoliated Graphite (EG) Preparation

Expanded graphite was prepared by graphite exfoliation [23]. A mixture of graphite, CrO_3 and HCl (1 g, 8.5 g and 7mL, respectively) was added into the 100 mL of aqueous solution. The solution was stirred at ambient temperature for 2 hours with magnetic stirrer. Then, the mixture was washed by distilled water until the remained chromium being precipitated. Finally, 10 mL of H_2O_2 was added to the solution and after 10 minutes, 10 mL was added again. Chromium which was diffused into the molecular structure of graphite resulted in graphite expansion. Expanded graphite was frozen with cold weather for being dry [24]. Figure 2 Shows natural graphite powder and EG.

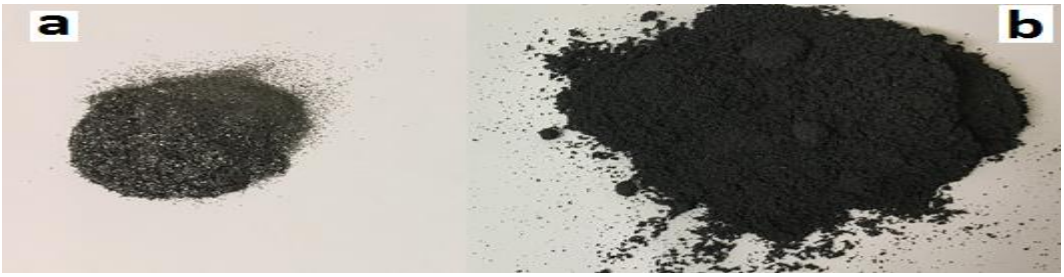

Figure 2. Natural graphite powder (a) and exfoliated graphite (b)

Sorption Experiments

The sorption capacities of EG for oils were evaluated following the test methods given in the standard ASTM F 726-99(25). Thus, a glass beaker was filled with 100 mL of water. An oil sample of the known weight (around 0.5 g) was added to the aqueous solution. Then an EG (0.02 g) was placed into the oily water liquid. After a few seconds, the absorbent loaded with oil was removed from liquid. Subsequently, it was weighted using a digital balance. The difference between the loaded and fresh absorbent gave the maximum sorption performance also known as the initial absorption capacity [25]:

$$S = \frac{W_{so} - W_s}{W_s} \quad (1)$$

Where S (g oil/g absorbent) denotes the sorption capacity, W_S (gr) shows the weight of fresh absorbent and W_{SO} (g) is the weight of loaded absorbent with oil. The sorption capacity test was carried out at room temperature.

Response surface methodology (RSM)

Absorption properties were investigated using response surface methodology. The Design of Experiment software 11.1.1.0-(Stat-Ease, Minneapolis, USA) was used for determining the central composite design of the experiment to calculate the 2 and 3D response surface and (ANOVA) analysis of variance [26-28]. Two independent, controllable and important parameters, weight of absorbent (g) and oil (g) were used to discuss absorption. The total domain for parameters was shown in Table 2.

Table 2. Total domain for absorption parameters

Parameters	Factor	Unit	Domain				
			-a	-1	0	+1	+a
Absorbent	A	g	0.0058	0.01	0.02	0.03	0.034
Oil	B	g	0.075	0.2	0.5	0.8	0.92

Instrumentation

The surface morphology of EG was characterized using a TESCAN (MIRA3) scanning electron microscope (SEM) used for taking the sample image. Energy dispersive X-ray spectroscopy (EDS) analysis was attained with a Philips Tecnai 20 electron microscope. Fourier transform infrared (FT-IR) spectra were recorded in the range of 400–4000 cm^{-1} on a RAYLEIGH WQF-510A FT-IR spectrophotometer using the KBr pellets. The Bel (Belsorp mini II Japan) was used for calculating of pore diameter and specific surface area with Brunauer–Emmet–Teller (BET) and Barrett–Joyner–Halenda (BJH) equations. RAMAN spectra were recorded on a TEKSAN (Takram N1-541) spectrophotometer. The crystalline structures of the products were evaluated by X-ray diffraction (XRD) analysis on a X'Pert Pro MPD diffractometer with Cu-K_α radiation (λ = 1.5418 Å) operated at 40 kV and 40 mA.

Results and discussion

Characterization of the absorbent

BET

The BET technique used for studying pore size distribution and surface properties of the synthesized materials by N_2 adsorption–desorption isotherms [29-30]. Adsorption-desorption isotherm of the EG is shown in fig. 3.a. The BET surface area of EG was98.8 m^2g^{-1}. The surface area of EG was higher than that of the simple graphite (10 times).The corresponding pore size distribution of the sample was calculated by the desorption branches of the isotherms using the BJH method. The pore size distribution curves (fig. 3.b) showed that the BJH desorption average pore size and the total pore volume of EG were about 5.83 nm and 0.113 cm^3g^{-1}, respectively, which is the characteristic of mesoporous material

with small pores and uniform channels. These results indicated that the large surface of product was efficiently imprinted. The BET analysis report is also shown in Table 3.

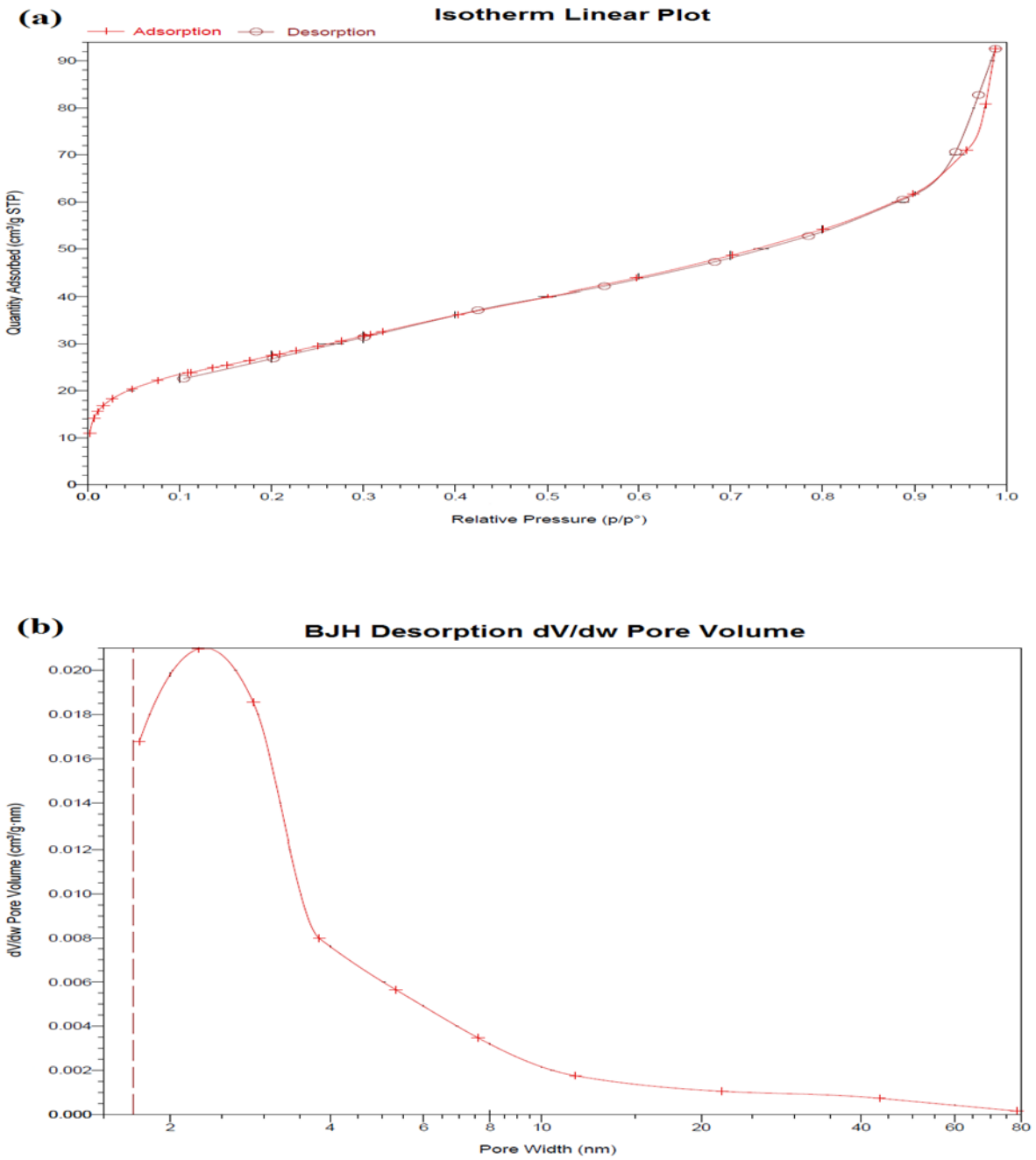

Figure 3. N_2 adsorption/desorption isotherms (a) and BJH desorption/pore size distribution (b)

Table 3. Obtained results of BET analysis

Absorbent	Surface Area $S_{BET}(m^2/g)$	Total Pore Volume $V_T(cm^3/g)$	Average Pore Size $W_{BJH}(nm)$
EG	98.8	0.113	5.83

SEM & EDS

The morphology of the EG was monitored by scanning electron microscopy. The SEM image of the EG was seen to swell and enlarge in thickness, giving rise to exfoliated products in significant quantities with a morphology of very thin, corrugated layers separated by micrometric or even nanometric voids (Figure 4). This morphology is the characteristic of delaminated graphite [31-32]. The energy dispersive spectroscopy (EDS) was used to the elemental analysis of EG. The strong presence of C and O were revealed, illustrated that carbon and oxygen are the major elements in synthesized structure. The weight (W %) and atomic (A %) percentages of C and O can be found in Table 4.

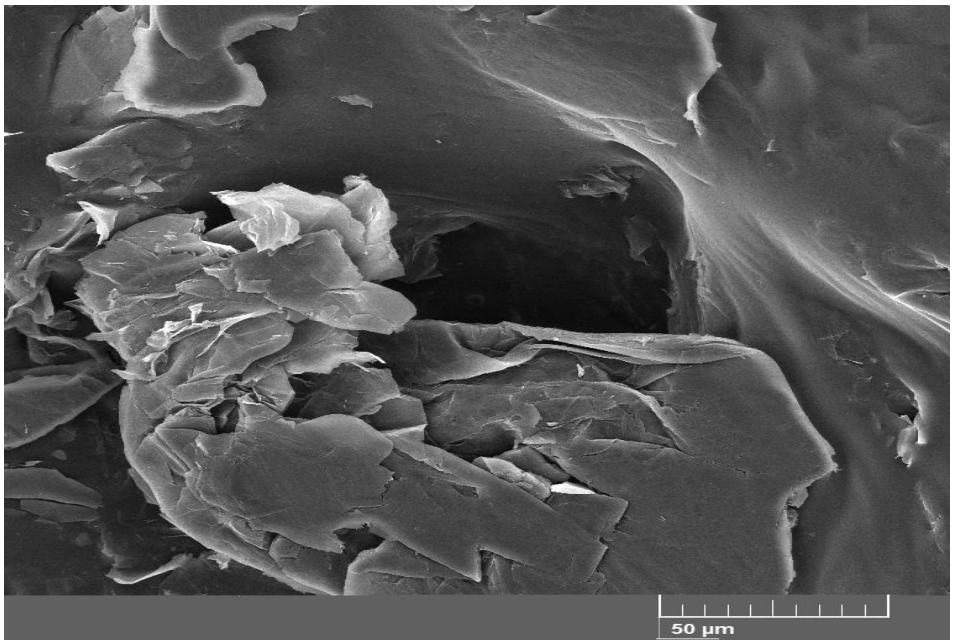

Figure 4. The SEM image of the EG

Table 4. Quantitative results of EDS spectra

Element	W%	A%
Carbon	59.88	66.54
Oxygen	40.12	33.46
Total	100.00	100.00

FT-IR

The Fourier-transform infrared spectroscopy (FTIR) spectra of the EGare shown in Figure 5. A broad peak, at about 3424 cm^{-1}, is assigned to the stretching vibration of the hydroxyl (O-H) band. The characteristic band of the C-H group is observed at 2800-2900 cm^{-1}. At around 1050 cm^{-1} was observed the stretching which is related to C-O-C band and the peak of 1640 cm^{-1} proves the existence of carbonyl (C-O) group stretching vibrations. Also the 2374 cm^{-1} peak caused by physically absorption of CO_2 molecules. Due to this characterization, confirmed the successfully EG surface [33].

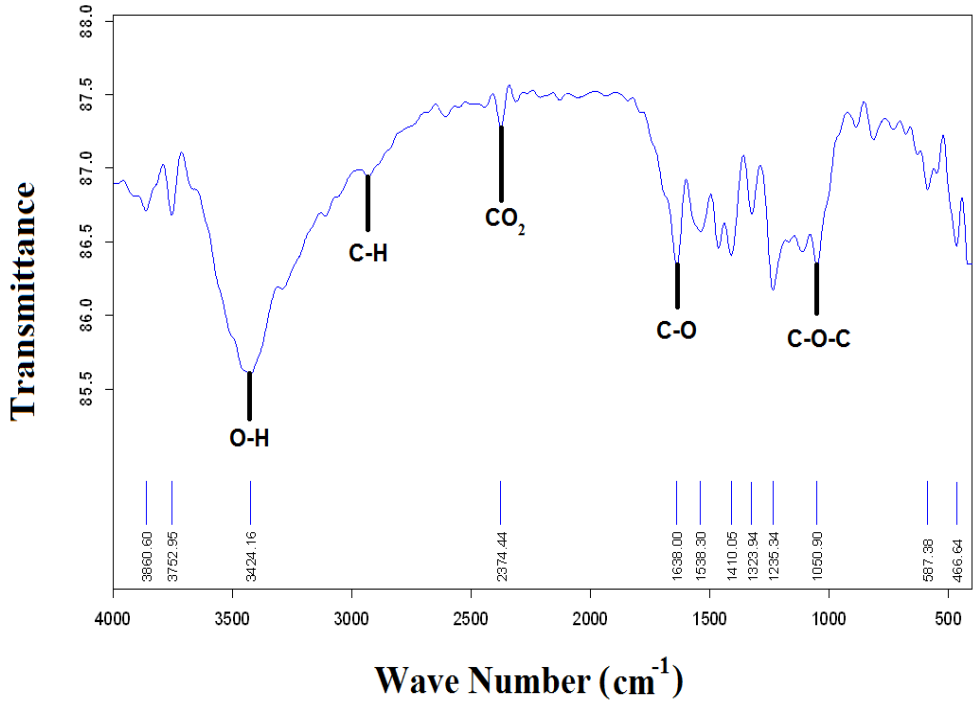

Figure 5. FTIR spectra of EG

XRD

In order to confirm and identify the ingredients, the exfoliated graphite (EG) was also investigated by XRD as compared to the XRD of simple graphite (SG). Figure 6a shows an X-ray diffraction result which clearly indicates typical graphite structure of the SG; a sharp diffraction line appears at $2\theta = 26.5^{\circ}$, demonstrating the presence of a crystalline structure with stacking layers of the graphite [34-35]. However, a broad diffraction line appears at XRD result of EG with a same angle (26.5°) (fig 6b) which shows that the crystalline structure of SG changed and turned lightly into amorphous structure as graphite became expanded.

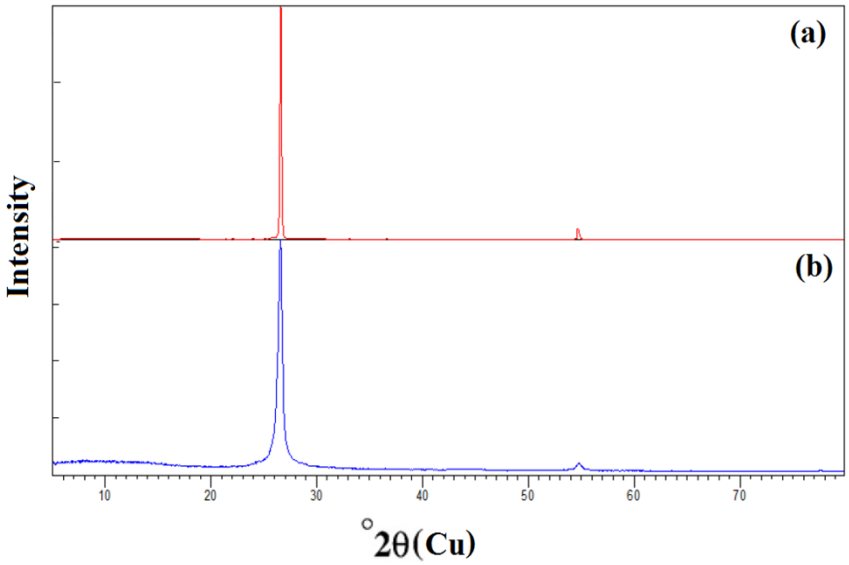

Figure 6. X-ray diffractogram of the SG (a) and EG samples (b)

RAMAN Spectroscopy

The exfoliation of graphite is also evidenced by Raman spectroscopy. The shift of the EG was normalized to the intensity of the D-band and G-band. Figure 7 exhibits the Raman shift of the EG and its characteristic bands: a low intensity D-band at 1350 $cm^{-1}$is observed and it was caused by the breathing mode of the sp^2 carbon atoms and activated by the existence of defects such as edges, functional groups, or structural disorders [36]. A G-band is shown at 1580 cm^{-1} and a 2D-band at 2700 cm^{-1}. 2D-band is intrinsically different from that of the simple graphite, indicating that the SG is highly exfoliated [37]. The intensity of the G-band is more than two times that of D-band so, the ratio of intensity of D-band to G-band (I_D/I_G), which is known as an estimation of the defect level [37-38], is calculated as 0.38, suggesting a low defect level for the EG.

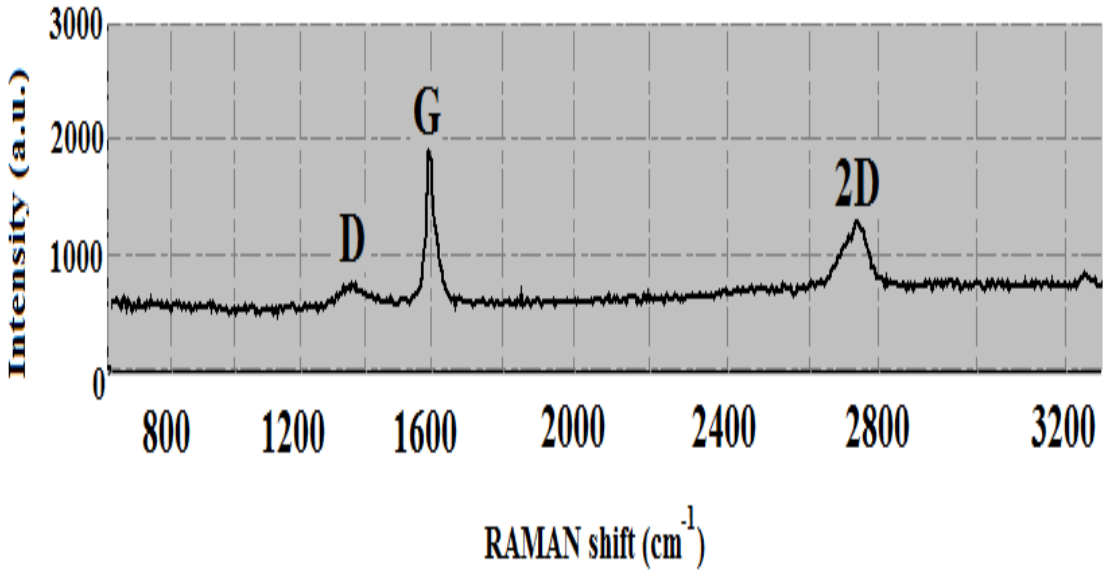

Figure 7. RAMAN spectra for EG

Response surface methodology (RSM)

RSM Modeling, Fitting and Statistical Analysis

The statistical analysis on the data is obtained using the analysis of variance table in order to determine the significance and effectiveness of the second degree model.

The result can be seen in Table 5. The ANOVA analysis table has defined the quadratic model statistically significant.

Table 5. ANOVA for response surface quadratic model for the response variables

Source of Variation	Sum of Squares	Degree of Freedom	Mean Square	F-value	p-value Probability
Model	587.42	5	117.48	590.96	< 0.0001
A-Absorbent	133.19	1	133.19	669.95	< 0.0001
B-oil	322.84	1	322.84	1623.92	< 0.0001
AB	30.97	1	30.97	155.78	< 0.0001
A^2	37.26	1	37.26	187.43	< 0.0001
B^2	75.27	1	75.27	378.62	< 0.0001
Residual	1.39	7	0.1988		
Lack of Fit	0.4516	3	0.1505	0.6406	0.6278
Pure Error	0.9400	4	0.2350		
Correction Total	588.81	12			
R^2	0.9976				
	0.9959				
Adjusted R^2	0.9921				
Predicted R^2					

The Model F-value of 590.96 implies that the model is significant. There is only a 0.01% chance that an F-value can occur due to noise. P-values less than 0.0500 indicate that model terms are significant. In this case A, B, AB, A^2, B^2 are significant model terms. The Lack of Fit F-value of 0.64 implies the Lack of Fit is not significant relative to the pure error. There is a 62.78% chance that a Lack of Fit F-value this large could occur due to noise. Non-significant lack of fit is good -- we want the model to fit. R^2 is the statistical parameter to measure how close the data and the fitted model are, in other words it is useful to determine the accuracy of the fitted model on the data. As the values become closer to 1, the fitted model becomes more capable of providing the results closer to the actual values, as a function of independent variables. The Predicted R^2 determines the accuracy of the model in predicting the results for the new observations. Thus, its higher values represent better prediction of the results. The adjusted R^2 is a developed version of R^2 which is always smaller than it and its value only increases if the improvement due to adding a new term is more than what is expected by chance. In order for the model make satisfactory predictions, the adjusted and predicted R^2 values should be close[39]. In this research the value of R^2 was 0.9976 which is very close to 1. Also the values of R^2_{adj} and R^2_{pred} were

0.9959 and 0.9921 respectively. Good agreement of these values represents the suitable fitting of the model using the software. Final equation in terms of Coded Factors is as follows:

Absorb=
+25.40
-4.08 A
+6.35 B
+2.78 AB
-2.31 A^2
-3.29 B^2 (2)

Which A and B represent absorbent and oil, respectively. The equation in terms of coded factors can be used to make predictions about the response for given levels of each factor. By default, the high levels of the factors are coded as +1 and the low levels are coded as -1. The coded equation is useful for identifying the relative impact of the factors by comparing the factor coefficients. In the diagnostic section of the design experiment software some provided diagrams could be applied to investigate the validity of the model. The section includes the analysis of normality of the experiment data, showing the residual for the predicted results and the level of closeness of the predicted results and the actual results. The normal probability diagram can be seen in Figure 8a, in which the plotted points close to the straight line prove the normal distribution of errors with an average value of zero. Another way to determine the sufficiency of the model is to study the residual which is shown in Fig. 8b, random scatters evenly distributed above and below the horizontal axis proves the sufficiency of the model. Also in Fig. 8c the values which were obtained from the presented model is compared with the values which were achieved from the actual results. The clustering of the points around the line indicates a satisfactory correlation between the experimental and predicted data, confirming the robustness of the model.

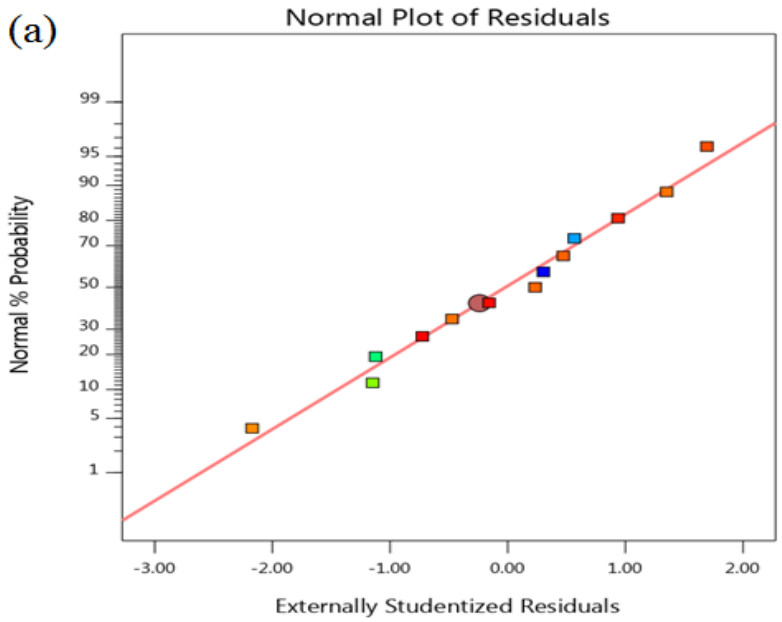

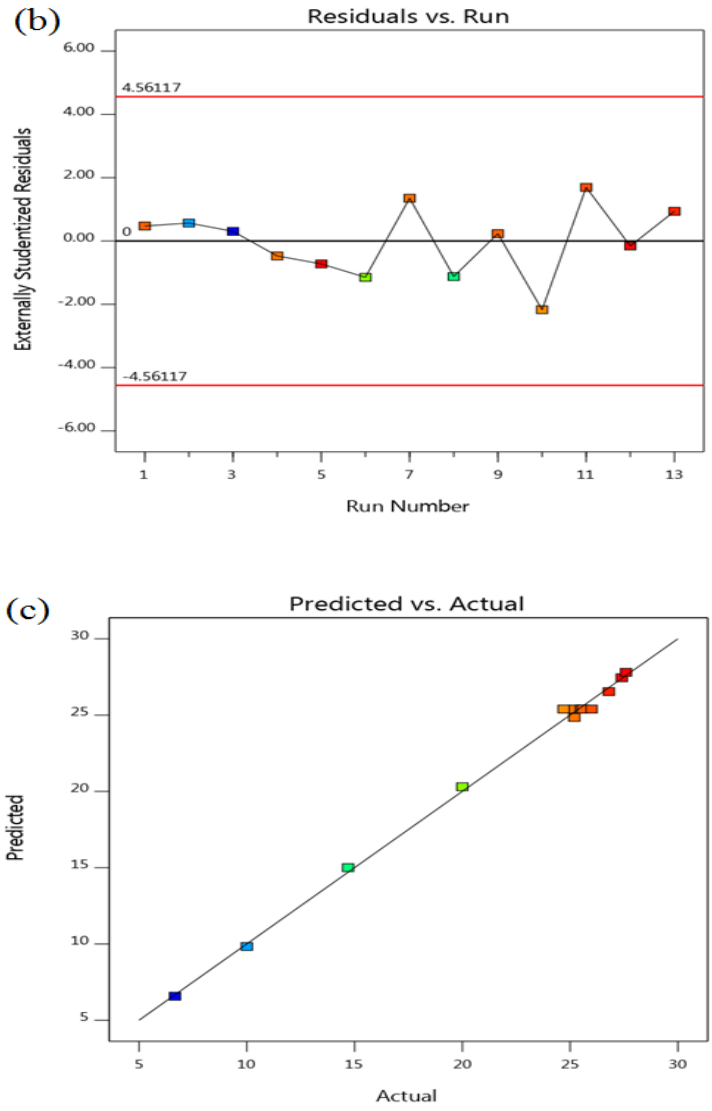

Figure 8. (a) Normal probability of residuals, (b) residuals vs. Run and (c) correlation of actual and predicted values by the model

Using RSM to determining the Absorption Capacity

The parameters (weight of EG and oil) were optimized using response surface methodology (RSM) to optimize the values of responses including absorption capacity. In the perturbation diagram presented in Fig. 9, the effects of the two parameters on oil absorption are shown. This diagram represents a general view of the effect of changing two parameters on the result. The influence of A (absorbent = 0.02 gr) and B (oil – 0.5 gr) for absorption capacity are almost different. In lower values, the influence of B is more impressive which demonstrate that absorption capacity is dependent to amount of oil more than amount of absorbent, but in higher values, absorbent effectiveness is more. The optimum value for two parameters is obvious, which means by making small changes in their values, the percentage absorption capacity of EG changes noticeably.

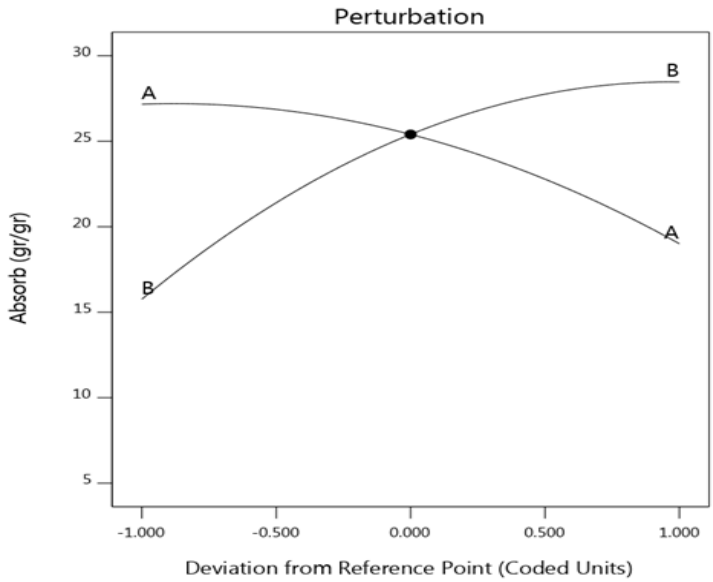

Figure 9. The perturbation diagram for the significant parameters in percentage of absorbent capacity in function of coded values, the coded values in the base point (code= 0) are: A: 0.02gr and B: 0.5gr

The contour and 3D surface response plots are used in order to determine the optimized value for the variables in which the result would be maximized [40]. In these diagrams the parameters influence and the interaction between two independent factors are illustrated. Figure 10a b shows the samples of the contour plot and 3D surface response for absorbent and oil. Each contour and surface response plot provides data on the interaction between two parameters. Figure 10a shows the two-dimensional response surfaces of EG absorption capacity and the relationship between A: absorbent (gr) and B: oil (gr) at the center point. It presents a simultaneous effect of A and B on the absorption capacity. Looking more closely to the figure, the maximum absorption capacity (27.6gB/gA) was observed for A=0.02 and B= 0552. (Figure 10b, showing 3D surface respond, has a similar interpretation).

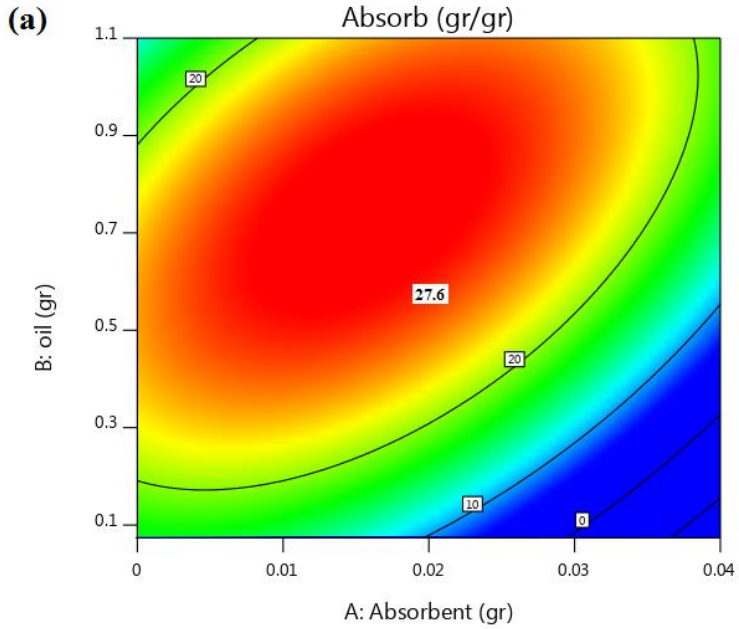

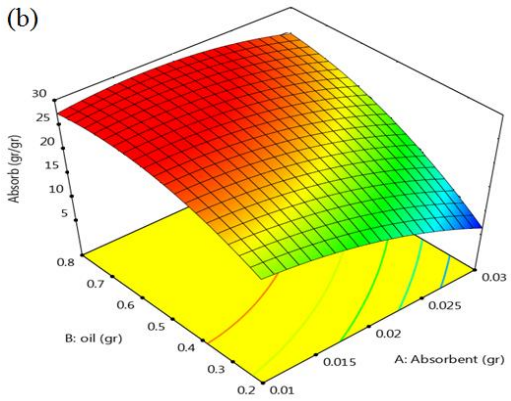

Figure 10. Contour plot (a) and 3DSurface response (b)for oil absorption capacity by EG

Conclusion

Exfoliated graphite, was synthesized by CrO_3(intercalation/expansion) and H_2O_2 via interlayer chemical reaction. The characterization of the EG was carried out by BET, SEM, EDS, FT-IR, XRD and RAMAN spectroscopy. The EG absorbent had good capacity for absorption of remained oil spill from Caspian Sea water. Response surface methodology was used for optimization of the absorption capacity by two effective parameters: weight of EG and oil (gr). RSM model fitting and statistical analysis was done by ANOVA results, R^2=0.9976which represents the suitable fitting of the model, final equation in terms of actual factors and diagnostic section of the design experiment software. Perturbation diagram, contour and 3D surface response plots were used to determine the optimized value for sorption. At the optimal conditions of absorption process, the proposed absorbent was used for the maximum sorption of 27.6 (gr oil/gr EG) from seawater sample. Exfoliated graphite, due to being easier to prepare, low cost and high performance in absorption instead of simple graphite and other carbon-based absorbents, could be an appropriate absorbent for oil spill from Caspian seawater.

Acknowledgments

The authors wish to thank faculty of environment, University of Tehran for support. Also we want to thank Khazar Exploration and Production Company (KEPCO) for supplying an oil sample which was explored from Caspian Sea.

References

[1] M. Hassanshahian, G. Emtiazi, S. Cappello, *Mar. Pollu. Bull*., **2012**, *64*, 7–12.
[2] X. Ding, R.Wang, X. Zhang, Y.Zhang, Sh. Deng, F. Shen, X. Zhang, H. Xiao, L. Wang, *Mar. Poll. Bull*., **2014**, *81*, 185–190.
[3] M.A. Lutfullin, O.N. Shornikova, A.V. Vasiliev, K.V. Pokholok, V.A. Osadchaya, M.I. Saidaminov, N.E. Sorokina, V. Avdeev, *CARBON*., **2014**, *66*, 417 – 425.
[4] F. Vafai, V. Hadipour, A. Hadipour, *Oce.&Coas. Manag*., **2013**, *71*, 123-130.
[5] G. Shirneshan, A. Bakhtiari, M. Memariani, *Mar. Poll. Bull*., **2017**, *115*, 383–390.
[6] A. Abesi, M. Saidi, *Jour. Env. Stud*., **2010**, *36*, 43-58.
[7] I-M. Efendiyeva, *Jour. Petr. Sci. Eng*., **2000**, *28*, 227–231.
[8] N. Pashayev, R. Ragimov, R. Samedov, D. Gahramanova, *IFAC PapersOnLine*., **2018**, *51*, 558–560.

[9] U. Farooq, I. Tabanb, P. Dalinga, *Mar. Poll. Bull*., **2018**, *135*, 119–128.
[10] Z. Rahmani, M. Samadi, A. Kazemi, A. Rashidi, A. Rahmani, *Jour. Env. Chem. Eng*., **2017**, *5*, 5025–5032.
[11] V. Makotchenko, E. Grayfer, A. Nazarov, S. Kim, V. Fedorov, *CARBON*., **2011**, *49*, 3233 –3241.
[12] Sh. Li, Sh. Tian, Y. Feng, J. Lei, P. Wang, Y. Xiong, *Jour. Haz. Mat*., **2010**, *183*, 506–511.
[13] P.Wang, T.Yao, B. Sun, X. Fan, S. Dong, Y. Bai, Y. Shi, *Coll and Surf A: Physicochem. Eng. Aspect*s., **2017**, *513*, 396–401.
[14] Z. Jijin, L. Xiaoxia, G. Yuxiang, M. Deyue, *Adv. Mat. Res*., **2014**, *852*, 101-105.
[15] T.Yao, Y.Zhang, Y. Xiao, P. Zhao, L. Guo, H. Yang, F. Li, *Jour. Mol. Liq*., **2016**, *218*, 611–614.
[16] M. Skowronski, *Jour. Mat. Sci*., **1988**, *23*, 2243-2246.
[17] A. Soubh, M. Baghdadi, M. Abdoli, B. Aminzadeh, *Jour. Env. Chem. Eng*., **2018**, *6*, 6568-6579.
[18] N. Sykam, N. Jayram, G. Rao, *Jour. Wat. Proc. Eng*., **2018**, *25*, 128–137.
[19] A. Azizi, E. Moniri, A. Hasani, H. Ahmadpanahi, F. Kahi, *Jour. Env. Stud*., **2018**, *44*, 1-15.
[20] S. Teixeira, C. Delerue-Matos, L. Santos, *Sci. Tot. Env*., **2018**, *646*, 168–176.
[21] H. Majdi, A. Esfahani, M. Mohebbi, *Com. Elec. Agr*., **2018**, *156*, 574–584.
[22] A. Ahmad, T. Otitoju, B. Ooi, *Jour. Tai. Ins. Chem. Eng*., **2018**, *93*, 461–476.
[23] Sh. Li, Sh. Tiana, Ch. Du, Ch. He, Ch. Cen, Ya. Xiong, *Chem. Eng. Jour*., **2010**, *162*, 546–551.
[24] M. Hassan, K. Reddy, E. Haque, A. Minett, V. Gomes, *Jour. Coll. Inter. Sci*., **2013**, *410*, 43–51.
[25] A. Rotaru, C. Cojocaru, I. Cretescu, M. Pinteala, D. Timpu, L. Sacarescu, V. Harabagiu, *Sep. Puri. Tech*., **2014**, *133*, 260–275.
[26] D. Sharma, K. Yadavb, S. Kumar, *Biores. Tech*., **2018**, *270*, 198–207.
[27] P. Choudhury, P. Mondal, S. Majumdar, S. Saha, G. Sahoo, *Jour. Clea. Prod*., **2018**, *203*, 511- 520.
[28] M. Shanmugaprakash, S. Venkatachalam, K. Rajendran, A. Pugazhendhi, *Jour. Env. Manag*., **2018**, *227*, 216–228.
[29] H. Vojoudi, A. Badiei, Sh. Bahar, Gh. Ziarani, F. Faridbod, M. Ganjali, *Pow. Tech*., **2017**, *319*, 271–278.
[30] H. Vojoudi, A. Badiei, Sh. Bahar, Gh. Ziarani, F. Faridbod, M. Ganjali, *Jour. Magn. MagMater*., **2017**, *441*, 193–203.
[31] J. Munuera, J. Paredes, S. Villar-Rodil, A. Castro-Mu˜niz, A. Martínez-Alonso, J. Tascón, *Appl. Mat. Tod*, **2018**, *11*, 246–254.
[32] Y. Hernandez, V. Nicolosi, M. Lotya, F. Blighe, Z. Sun, *Nat. nanotech*., **2008**, *3*, 563-568.
[33] A. Iona, A. Alpatovab, I. Iona, A. Culetu, *Mat. Sci. Eng*., **2011**, *176*, 588–595.
[34] K. Takeuchi, M. Fujishige, H. Kitazawa, N. Akuzawa, J. Medina, A. Morelos-Gomez, R. Silva, T. Araki, T. Hayashi, M. Terrones, *Jour. Wat. Proc. Eng*., **2015**, *8*, 91–98.
[35] G. Wang, Q. Sun, Y. Zhang, J. Fan, M. Luming, *Desalination*., **2010**, *263*, 183–188.
[36] Kh. Parvez, Zh.Wu, R. Li, X.Liu, R. Graf, X. Feng, K. Müllen, *Jour. Amer. Chem. Soci*., **2014**, *136*, 6083−6091.
[37] Sh. Liang, Z. Shen, M. Yi, L. Liu, X. Zhang, S. Ma, *Carbon*., **2016**, *96*, 1181-1190.
[38] K. Takeuchi, H. Kitazawa, M. Fujishige, N. Akuzawa, J. Medina, A. Morelos-Gomez, R. Silva, T. Araki, T.

Hayashi, M. Terrones, *Jour. Wat. Proc. Eng*., **2017**, *20*, 226–231.
[39] T. Najib, M. Solgi, A. Farazmand, M. Heydarian, B. Nasernejad, *Jour. Env. Chem. Eng*., **2017**, *5*, 3256–3265.
[40] S. Yavari, A. Malakahmad, N. Sapari, S. Yavari, *Proc. Saf. Env. Prot*., **2017**, *109*, 509–519.

How to cite this manuscript: Omid Ghasemi, Naser Mehrdadi, Majid Baghdadi, Behnoosh Aminzadeh. An investigation on absorption properties of exfoliated graphite for oil spill from Caspian Sea water. *Iranian Chemical Communication*, 2019, 7(4), 352-367.